

CALCITE – AMPHIBOLE – CLINOPYROXENE ROCK FROM THE AFRIKANDA COMPLEX, KOLA PENINSULA, RUSSIA: MINERALOGY AND A POSSIBLE LINK TO CARBONATITES. II. OXYSALT MINERALS

ANATOLY N. ZAITSEV[§]

Institut für Mineralogie, Petrologie und Geochemie, Universität Freiburg, Albertstr. 14a, D-79104 Freiburg, Germany

ANTON R. CHAKHMOURADIAN

Department of Geological Sciences, University of Manitoba, 125 Dysart Road, Winnipeg, Manitoba R3T 2N2, Canada

ABSTRACT

Carbonate – amphibole – clinopyroxene rocks and carbonatites from the Afrikanda complex, in the Kola Peninsula, Russia, contain a number of oxysalt minerals, including major calcite (15–95 vol.%), subordinate hydroxylapatite, ancylite-(Ce), calcio-ancylite-(Ce), and minor burbankite, khanneshite, nyerereite, shortite, bradleyite, strontianite, britholite-(Ce) and barite. Three mineral parageneses differing in the mode of occurrence of calcite are distinguished: (1) calcite – magnesiohastingsite – diopside rock, (2) segregations of perovskite and titanite, and (3) calcite carbonatite. Cathodoluminescence studies document a complex evolutionary history of primary Sr-enriched calcite (0.6–1.4 wt.% SrO) involving late-stage resorption and replacement by a low-Sr variety (<0.5 wt.% SrO). The presence of nyerereite, shortite, bradleyite, burbankite and khanneshite as solid inclusions in the early-crystallized minerals (primarily oxides and hydroxylapatite) indicates initially high activities of Na in the system. The transition from nyerereite (inclusions in magnetite) to shortite (in perovskite) signifies evolution of the carbonatite system toward Ca-enriched compositions. Crystallization of ancylite-(Ce) and calcio-ancylite-(Ce) is related to low-temperature hydrothermal processes, whereas burbankite and khanneshite probably represent primary magmatic phases. Low-temperature (200–250°C) hydrothermal alteration accompanied by isotope-exchange processes produced variations in the oxygen isotopic composition of the Afrikanda rocks ($\delta^{18}\text{O}$ in the range 9.3 to 12.1‰ SMOW). Subtle variations in the isotopic composition of carbon ($\delta^{13}\text{C}$ in the range –2.5 to –1.7‰ PDB) suggest interaction with a meteoric-hydrothermal fluid with a low $\text{CO}_2\text{:H}_2\text{O}$ ratio. The observed high $\delta^{13}\text{C}$ values of the calcite are consistent with heterogeneity of the mantle beneath the Kola Craton; the heterogeneity probably was due to a subduction-related source of contamination.

Keywords: calcite, ancylite-(Ce), calcio-ancylite-(Ce), burbankite, khanneshite, nyerereite, shortite, bradleyite, C–O isotopic composition, Raman spectroscopy, carbonatite, Afrikanda, Kola Peninsula, Russia.

SOMMAIRE

Les roches à carbonate – amphibole – clinopyroxène et les carbonatites du complexe igné d’Afrikanda, péninsule de Kola, en Russie, contiennent plusieurs oxysels parmi les minéraux représentés. En plus de la calcite, phase majeure (15–95% par volume), on trouve des quantités moindres d’hydroxylapatite, d’ancylite-(Ce) et de calcio-ancylite-(Ce), ainsi que des quantités mineures de burbankite, khanneshite, nyérérite, shortite, bradleyite, strontianite, britholite-(Ce) et barite. Nous distinguons trois paragenèses de minéraux selon le rôle de la calcite: (1) roche à calcite – magnesiohastingsite – diopside, (2) ségrégations de pérovskite et de titanite, et (3) carbonatite à calcite. Nos études par cathodoluminescence documentent une évolution complexe de la calcite primaire enrichie en Sr (0.6–1.4% SrO, base pondérale), qui subit une résorption tardive et un remplacement par une variante appauvrie en Sr (<0.5% SrO). La présence de nyérérite, shortite, bradleyite, burbankite et khanneshite incluses dans les minéraux précoces (surtout dans les oxydes et l’hydroxylapatite) indique une activité élevée de sodium au départ dans le système. La transition de nyérérite (en inclusion dans la magnétite) à shortite (dans la pérovskite) signale l’évolution de la carbonatite vers des compositions davantage enrichies en Ca. La cristallisation de l’ancylite-(Ce) et de la calcio-ancylite-(Ce) est liée aux processus hydrothermaux à faible température, tandis que la burbankite et la khanneshite représenteraient des phases magmatiques primaires. Une altération hydrothermale à faible température (200–250°C) accompagnée d’un échange isotopique est responsable des variations dans la composition isotopique de l’oxygène des roches d’Afrikanda ($\delta^{18}\text{O}$ dans l’intervalle de 9.3 à 12.1‰ SMOW). Des variations subtiles de la composition isotopique du carbone ($\delta^{13}\text{C}$ dans l’intervalle de –2.5 à –1.7‰ PDB) seraient dues à une

[§] *Permanent address:* Department of Mineralogy, St. Petersburg State University, 7/9 University Emb., St. Petersburg, 199034, Russia; *e-mail address:* anatoly@az1562.spb.edu

interaction avec une phase fluide météorique-hydrothermale ayant un faible rapport $\text{CO}_2:\text{H}_2\text{O}$. Les valeurs élevées de $\delta^{13}\text{C}$ de la calcite concordent avec l'hypothèse d'une hétérogénéité du manteau en dessous du craton de Kola. Cette hétérogénéité serait probablement due à une source de contamination liée à la subduction.

(Traduit par la Rédaction)

Mots-clés: calcite, ancyllite-(Ce), calcio-ancyllite-(Ce), burbankite, khanneshite, nyérérite, shortite, bradleyite, composition isotopique C–O, spectroscopie de Raman, carbonatite, Afrikanda, Peninsule de Kola, Russie.

INTRODUCTION

Oxysalt minerals (primarily carbonates, phosphates and sulfates) are major rock-forming or principal accessory constituents of carbonatites and genetically related rocks, including phoscorites (forsterite + apatite + magnetite + calcite or dolomite) and various silicate-carbonate (\pm quartz) rocks. Whereas *bona fide* phoscorites are rocks of undoubtedly magmatic origin, silicate-carbonate rocks may be produced by a variety of processes, including crystallization from a silica-rich carbonatitic magma, alkali metasomatism of ultramafic, foidolitic or melilitic wallrocks, and crystallization from late-stage CO_2 -rich hydrothermal fluids typically associated with carbonatitic magmatism. Knowledge of the chemical and isotopic composition of oxysalt minerals is important for assessment of the geochemical evolution of carbonatites and related rocks, the nature of their source(s) and degree of post-emplacement alteration (e.g., Le Bas & Handley 1979, Egorov 1984, Clarke *et al.* 1992, Buckley & Woolley 1990, Wall *et al.* 1994, Zaitsev & Bell 1995, Zaitsev 1996, Zaitsev *et al.* 1998).

In this paper, we report the results of mineralogical and C–O isotopic study of oxysalt minerals from calcite – amphibole – clinopyroxene rocks of the Afrikanda ultramafic-alkaline complex in the Kola Alkaline Province, northwestern Russia. This work continues a series of contributions concerned with the mineralogy and petrology of this unusual suite of rocks, and its possible linkage with carbonatites. The geology of the Afrikanda complex and the setting of calcite – amphibole – clinopyroxene rocks (CAPR) have been described in detail by Kukharensko *et al.* (1965) and, more recently, by Chakhmouradian & Zaitsev (1999).

ANALYTICAL METHODS

Most of the mineral compositions were determined by energy-dispersion X-ray spectrometry (EDS) using a Hitachi 570 scanning-electron microscope equipped with a LINK ISIS analytical system incorporating a Super ATW Light Element Detector (133 eV FwHm MnK) at Lakehead University (Thunder Bay, Ontario). EDS spectra were acquired for 150–180 seconds (live time) with an accelerating voltage of 20 kV and a beam current of 0.84–0.86 nA. The spectra were processed with the LINK ISIS-SEMQUANT software package,

with full ZAF corrections. The data for calcite, ancyllite-(Ce) and calcio-ancyllite-(Ce) were cross-checked by wavelength-dispersion spectrometry (WDS) using a Cameca SX-50 electron microprobe located in the Natural History Museum (London, U.K.). The microprobe was operated at 15 kV and 15 nA, with a spot size of 10 μm . Well-characterized minerals and synthetic materials were used as standards for both EDS and WDS. Concentrations of individual rare-earth elements (*REE*) were determined using *REE*-Ca–Al silicate glasses for WDS and naturally occurring loparite-(Ce) for EDS. In the latter case, element profiles were obtained from synthetic fluorides of individual *REE*. The X-ray element-distribution maps were obtained using a Zeiss DSM 960 scanning electron microscope equipped with a Link ISIS analytical system (Freiburg University, Germany).

Cathodoluminescence studies were done using polished thin sections in a vacuum chamber of a cold-cathode electron gun (Technosyn Model 8200 MK II) mounted on a polarizing microscope (Freiburg University).

Carbon dioxide released from the calcite reacted at 25°C with 100% H_3PO_4 (McCrea 1950) was analyzed using a VG-ISOGAS SIRA-12 fully automated, fixed triple-collector mass spectrometer at the University of Ottawa (Ontario). For this instrument, the precision in determination of $\delta^{13}\text{C}$ and $\delta^{18}\text{O}$ is $\pm 0.1\%$. The fractionation factor used for the calcite- CO_2 pair is 1.01025 for at 25°C (Sharma & Clayton 1965, Friedman & O'Neil 1977).

For identification of some minerals, we employed confocal laser Raman spectroscopy using a LabRam microspectrometer (Jobin Yvon, formerly Dilor) with a He-Ne laser (Institute of Physical Chemistry, Karlsruhe University, Germany). The calibration of the Raman spectra was done using a Si standard and Rayleigh scattering of monochromatic light emitted by the laser. The counting time was 10 s for all samples. Raman spectroscopy has been effectively used for identification of minerals, particularly those that occur as inclusions that are too small for a routine X-ray-diffraction study (e.g., Burke 2001). In CAPR, a number of minerals form solid inclusions (captured crystals and solidified melt inclusions) in hydroxylapatite, magnetite, perovskite and ilmenite. Their maximum size does not exceed 50 μm . The inclusions are represented by Na–Ca–Sr–Ba–*REE*,

Na–Ca and Na–Mg–P phases. The very low analytical totals obtained for these minerals using X-ray spectrometry suggest that they contain a significant proportion of CO_2 and, possibly, H_2O . For all of these minerals, recalculated atomic proportions of cations are nonstoichiometric owing to rapid decomposition of minerals under the electron beam and loss of Na, and in some cases, to the presence of vacancies in the structure. On the basis of the electron-microprobe data, we tentatively identified the inclusions as minerals of the burbankite group, alkali carbonates (e.g., H_2O -free nyerereite and shortite, or H_2O -bearing pirssonite and gaylussite), and the alkali phosphate–carbonate bradleyite.

Confocal laser Raman spectroscopy was used for more accurate identification of minerals in polished thin sections and slabs, following the procedure described by Böhn *et al.* (1999) for burbankite. Raman spectra were obtained for a set of standards that had been previously thoroughly examined by X-ray diffraction and electron-microprobe analysis. The reference spectra were then compared with those for the problematic Afrikanda minerals.

Spectra of burbankite-type minerals from Khibina and Vuoriyarvi (Kola Peninsula) were compared with those of the Na–Ca–Sr–Ba–REE phases in hydroxyl-apatite (Fig. 1a). The reference spectra are characterized by a strong peak at 1077 cm^{-1} (khanneshite), 1079 cm^{-1} (calcio-burbankite) and 1080 cm^{-1} (burbankite). In addition, there are weak satellite peaks at 707 , 704 and 710 cm^{-1} , and a broad band between 130 and 300 cm^{-1} , with maxima at about 165 , 227 and 275 cm^{-1} , respectively. The burbankite-group minerals from Afrikanda produce a similar pattern, with the strongest peak positioned at $1078\text{--}1079\text{ cm}^{-1}$.

The Raman spectra of two Na–Ca phases from Afrikanda were compared with those of nyerereite and gregoryite (Oldoinyo Lengai, Tanzania), shortite (Vuoriyarvi), pirssonite (Khibina and California: BM1972,206) and gaylussite (South Africa: BM1929, 1569), where the numerical symbols correspond to sample numbers in the collection of The Natural History Museum in London, U.K. The mineral occurring as inclusions in perovskite was identified as shortite, $\text{Na}_2\text{Ca}_2(\text{CO}_3)_3$ (Fig. 1b). On its spectrum, the main Raman shifts are at 1071 and 1090 (strong lines), 137 , 168 , 196 and 254 (weak lines), 717 and 730 cm^{-1} (very weak lines). Both the strongest and weak peaks are identical to those for the Vuoriyarvi material within a deviation of $\pm 1\text{ cm}^{-1}$. Accurate identification of the other Na–Ca phase (inclusions in magnetite) was hindered by fluorescence effects masking its Raman scattering. However, we were able to observe weak bands between 1074 to 1088 cm^{-1} , confirming the dominance of carbonate in this mineral; the absence of peaks in the range $3000\text{--}4000\text{ cm}^{-1}$ strongly suggests that the mineral is anhydrous. From these observations and the Na:Ca atomic ratio near $1.6\text{--}1.7$, we interpret these inclusions to represent nyerereite, $\text{Na}_2\text{Ca}(\text{CO}_3)_2$.

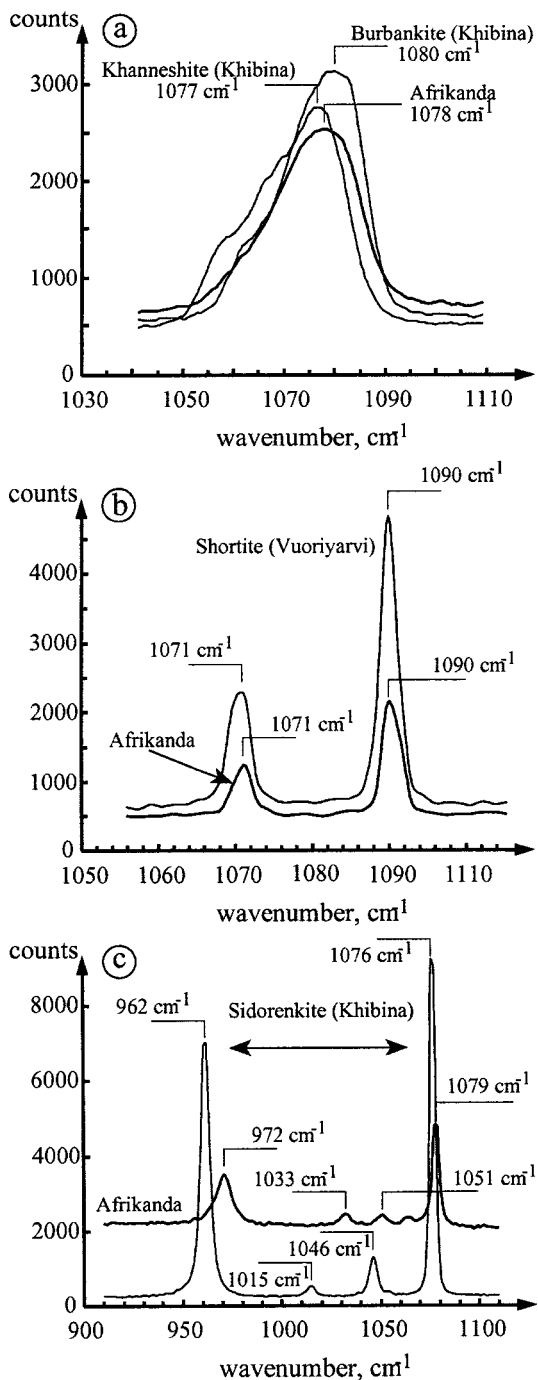


FIG. 1. Confocal Raman spectra of reference samples and inclusions of Na-bearing carbonates: (a) burbankite-group minerals, (b) shortite, and (c) bradleyite-type minerals.

Unfortunately, we were unable to locate a standard sample of bradleyite, $\text{Na}_3\text{Mg}(\text{PO}_4)(\text{CO}_3)$, and hence, used sidorenkite from the Lovozero complex (Kola) for identification of the Na–Mg–P phase from CAPR (Fig. 1c). Sidorenkite is the Mn-analogue of bradleyite, and the two minerals are isostructural (Chin Tkhi Le Tkhy *et al.* 1984). The Raman spectra of the sidorenkite and Na–Mg–P phase are similar, with strong lines at 962 and 972 cm^{-1} [$(\text{PO}_4)^{3-}$ active Raman species], as well as at 1076 and 1079 cm^{-1} [$(\text{CO}_3)^{2-}$ active Raman species], respectively. This similarity suggests that the Na–Mg–P phase from Afrikanda is indeed bradleyite.

OXYSALT MINERALS

The following six minerals comprise the bulk of CAPR: diopside, magnesiohastingsite, calcite, magnetite, perovskite and titanite. Other phases (in total, about 50 mineral species) together comprise only about 1 to 5% of the rock by volume. In this work, we distinguish three mineral parageneses, differing primarily in the mode of occurrence of calcite and its relationships with other phases: (1) an aggregate of calcite, magnesiohastingsite and diopside making up the bulk of the rock, with subordinate amounts of magnetite and perovskite, (2) coarse-grained to pegmatitic segregations of calcite, perovskite, magnetite and titanite, and (3) monomineralic veins of calcite in a cross-cutting relationship with parageneses (1) and (2).

Calcite

Calcite is the most common oxysalt mineral in CAPR. Its proportion may locally reach 15 vol.% of the rock in paragenesis (1), and up to 50 and 95 vol.% in parageneses (2) and (3), respectively. In all cases, the mineral typically occurs as white euhedral to subhedral crystals from 1 to 10 mm across, commonly arranged in a mosaic pattern with triple junctions at about 120° . The associated minerals (diopside, magnesiohastingsite, perovskite, magnetite and titanite) are invariably euhedral with respect to calcite. In association with perovskite and titanite [paragenesis (2)], calcite also occurs in pale violet or clear colorless varieties, and forms rhombohedral crystals in cavities [parageneses (2) and (3)].

Cathodoluminescence studies revealed a complex pattern of growth. In paragenesis (1), calcite exhibits simple zoning with an orange-yellow core and a red rim; both core and rim are relatively homogeneous, but locally, a subtle auxiliary zoning can be seen as well (Fig. 2a). Calcite from paragenesis (2) shows complex zoning. Commonly, it has an orange-yellow core surrounded by a zone with a yellow, orange-yellow, red, dark red or green-yellow luminescence. The rim of the crystals is characterized by an irregular or, in some cases, oscillatory-type zoning, and has embayed contacts with the core, suggestive of a resorption episode

during growth (Fig. 2b). In addition, thin veinlets of calcite with a yellow or red color of luminescence are observed along the cleavage in the zoned crystals of calcite. The calcite from monomineralic veins forms homogeneous crystals of yellow or red-yellow luminescence cross-cut by calcite veinlets with red or dark red luminescence (Fig. 2c). The rhombohedral crystals from cavities normally exhibit a regular pattern of zoning indicative of uninterrupted growth (Fig. 2d). These observations illustrate the complexity of the crystallization history of calcite at Afrikanda. Whereas calcite in paragenesis (1) formed under relatively stable conditions in a closed system environment, the formation of perovskite and titanite in paragenesis (2) was followed by partial dissolution of the primary calcite [paragenesis (1)] and its subsequent overgrowth by a new generation of calcite. Thin veins and veinlets cross-cutting and replacing the earlier-formed crystals are clearly the latest generation of calcite to crystallize; their morphological features suggest a secondary origin. BSE imagery confirms the internal heterogeneity of the calcite crystals. Euhedral crystals of calcite contain elongate (1–20 μm wide) and patchy areas (up to 0.2 mm across) of lower average atomic number (AZ) than the primary calcite. These areas are normally confined to cleavages, and are similar in morphology to those shown in Figure 2c.

The calcite from CAPR shows a noticeable variation in terms of its Sr content (0–1.4 wt.% SrO). The Mg, Mn and Fe contents are very minor, and none of the respective oxides attain concentrations above 0.3 wt.%. Ba was detected only in about a quarter of the 120 analyses made; its maximum concentration is 0.5 wt.% BaO (Table 1). Low levels of Sr (<0.5 wt.% SrO) characterize low-AZ zones, whereas comparatively higher-AZ (primary) areas contain between 0.6 and 1.4 wt.% SrO. Neither primary nor secondary calcite shows any significant variation in Sr content in the different parageneses. Sr-enrichment is generally characteristic of primary calcite in carbonatites worldwide; secondary or late-stage calcite invariably shows some depletion in Sr that is in some cases accompanied by enrichment in Mn (*e.g.*, Pouliot 1970, Sokolov 1985, Clarke *et al.* 1992, Dawson *et al.* 1996, Zaitsev 1996). The pale violet and colorless varieties of calcite, as well as the crystals from cavities, show very low Sr contents (<0.2 wt.% SrO), in accord with their late-stage origin.

Ancylite-group minerals

These minerals are common accessory phases in all three parageneses. We distinguish the following three morphological types of these minerals: (i) minute anhedral grains (5–100 μm across) in low-Sr veinlets and patches of calcite, (ii) large (up to 2 mm) prismatic euhedral crystals lining cavities in an aggregate of magnesiohastingsite, diopside, perovskite and titanite (Fig. 3) and filling fractures within perovskite and some

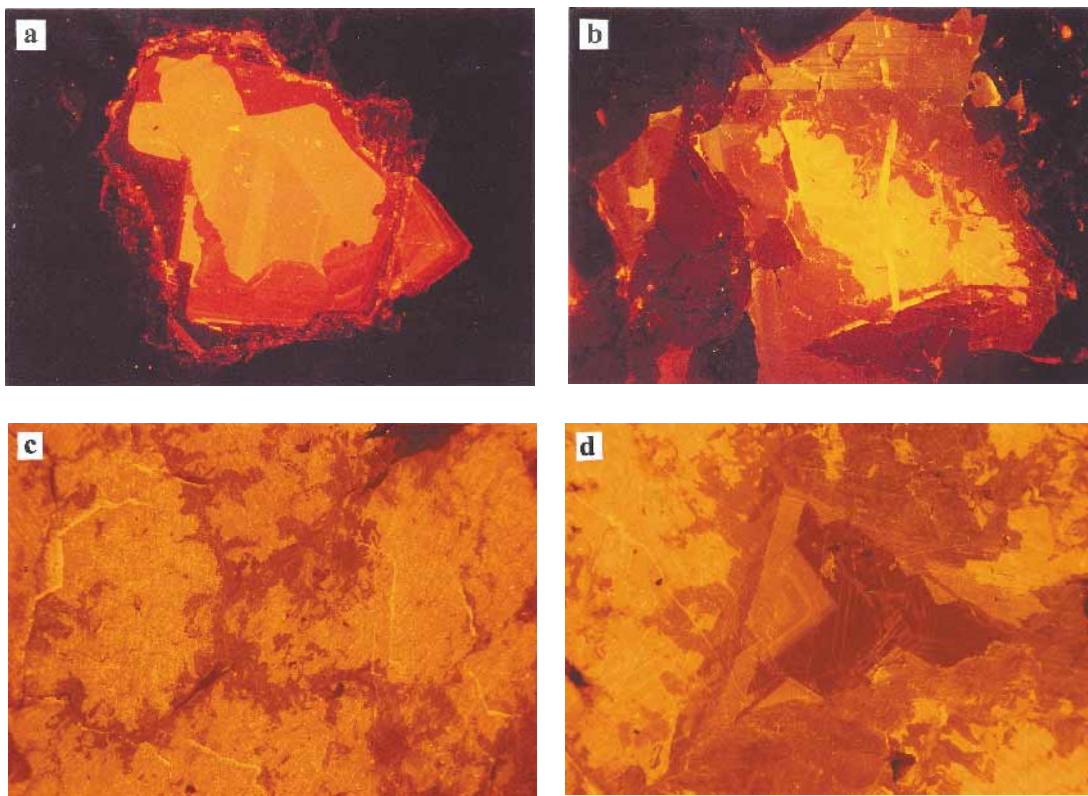


FIG. 2. Cathodoluminescence images showing (a) simple zoning in primary calcite from CAPR, (b) complex zoning in calcite from a perovskite-titanite segregation, (c) fine veinlets and irregular patches of late-stage calcite along the boundaries of larger crystals, and (d) cavity filled with euhedral crystals of late-stage calcite. Field of view: 3 mm.

silicate phases, and (iii) a thin rim (<20 μm in thickness) on prismatic hydroxylapatite (Fig. 4). The crystals of type (i) are associated with strontianite and barite, and those of type (ii), with cerite-(Ce), loparite-(Ce), titanite and ilmenite.

Euhedral crystals of ancylite – calcio-ancylite-(Ce) associated with perovskite from “ore nests in dark green pyroxenite” [our paragenesis (2)] have been studied by Pekov *et al.* (1997). These authors have demonstrated that Sr-rich compositions (Sr:Ca in the range 2.5–3.0) crystallized first, and the Sr:Ca ratio progressively decreased to 0.5 in a rim composed of calcio-ancylite-(Ce). Our data, incorporating results of 46 electron-microprobe analyses, show that the anhedral grains associated with the low-Sr calcite are invariably represented by ancylite-(Ce) (Table 2, anal. 1–3), whereas the euhedral crystals of type (ii) are zoned from ancylite-(Ce) in the core to calcio-ancylite-(Ce) in the rim (Table 2, anal. 4–6, Fig. 5), or are composed entirely of the latter mineral (Table 2, anal. 7–9). The ancylite-(Ce) and calcio-ancylite-(Ce) from Afrikanda are character-

ized by highly variable proportions of major components (1.2–10.2 wt.% CaO, 3.3–20.3 wt.% SrO and 44.7–60.5 wt.% REE_2O_3 ; Fig. 6); both minerals also contain appreciable amounts of Ba (up to 2.4 wt.% BaO) and F (1.2–1.3 wt.%). Some calcio-ancylite-(Ce) crystals are characterized by unusually high levels of Th, *i.e.*, 2.0–6.6 wt.% ThO_2 (Table 2, anal. 10). Both ancylite-(Ce) and calcio-ancylite-(Ce) are strongly enriched in light *REE* relative to heavy *REE* and Y, whose levels are below the detection limits. In all our samples, Ce is the dominant lanthanide; hence, the minerals should be referred to as ancylite-(Ce) and calcio-ancylite-(Ce).

The Sr:Ca ratio varies between 0.2 and 7.6, and the (Ca + Sr):*REE* ratio, between 0.4 and 0.9. In contrast to the findings of Pekov *et al.* (1997), we observed no correlation among the Sr/Ca, La/ Σ *REE* and Nd/ Σ *REE* values over the range of compositions obtained in this study. However, a weak positive correlation between the Sr/Ca and La/ Σ *REE* values, and a weak negative one between the Sr/Ca and Nd/ Σ *REE* values, are observed

TABLE 1. REPRESENTATIVE COMPOSITIONS OF CALCITE FROM AFRIKANDA (WT.%)

Point	1		2		3		4		5		6		7		8		10		11		12		13	
	host calcite		veinlets		host calcite		veinlets		host calcite		veinlets		host calcite		veinlets		host calcite		veinlets		host calcite		veinlets	
MgO	0.13	0.16	nd	nd	0.25	0.18	nd	nd	0.07	nd	0.10	nd	nd	0.07	nd	0.10	nd	0.07	nd	0.10	nd	0.10	nd	
CaO	54.29	54.13	56.43	56.38	54.32	54.52	55.95	56.18	53.15	54.39	54.28	54.28	54.28	53.15	54.39	54.28	54.28	53.15	54.39	54.28	54.28	54.28	54.28	
MnO	0.10	nd	0.05	nd	nd	nd	0.11	0.10	0.06	0.16	nd	nd	0.06	0.16	nd	nd	0.06	0.16	nd	nd	nd	0.06	0.06	
FeO	0.10	0.11	nd	nd	0.07	nd	nd	nd	0.20	0.05	0.09	nd	0.20	0.05	0.09	nd	0.20	0.05	0.09	nd	0.09	nd	nd	
SrO	1.41	1.32	0.18	0.15	1.18	1.10	0.17	0.14	1.10	0.75	0.49	0.19	1.10	0.75	0.49	0.19	1.10	0.75	0.49	0.19	0.49	0.19	0.19	
BaO	nd	0.10	0.07	0.11	0.09	0.10	nd	nd	nd	nd	nd													
Total	56.03	55.82	56.73	56.64	55.91	56.01	56.22	56.38	54.68	55.19	54.96	54.53	54.68	55.19	54.96	54.53	54.68	55.19	54.96	54.53	54.96	54.53	54.53	
Formulae based on 1 CO ₃ ²⁻ group																								
Mg	0.003	0.004			0.006	0.004			0.002		0.003			0.002		0.003			0.002		0.003		0.003	0.003
Ca	0.981	0.980	0.997	0.998	0.980	0.982	0.997	0.998	0.982	0.992	0.991	0.997	0.982	0.992	0.991	0.997	0.982	0.992	0.991	0.997	0.991	0.997	0.997	0.997
Mn	0.001		0.001				0.002	0.001	0.001	0.002			0.002				0.002						0.001	0.001
Fe	0.001	0.002			0.001				0.003	0.001	0.001		0.003	0.001	0.001		0.003	0.001	0.001				0.001	0.001
Sr	0.014	0.013	0.002	0.001	0.012	0.011	0.002	0.001	0.011	0.007	0.005	0.002	0.011	0.007	0.005	0.002	0.011	0.007	0.005	0.002	0.005	0.002	0.002	0.002
Ba		0.001		0.001	0.001	0.001																		
Total	1.000	1.000	1.000	1.000	1.000	1.000	1.000	1.000	1.000	1.000	1.000	1.000	1.000	1.000	1.000	1.000	1.000	1.000	1.000	1.000	1.000	1.000	1.000	1.000

1-4 paragenesis (1); 5-8 paragenesis (2); 10-13 paragenesis (3). Nd = not detected; total Fe expressed as FeO. Compositions 1-4 were obtained using WDS, and 5-13 using ED spectrometry.

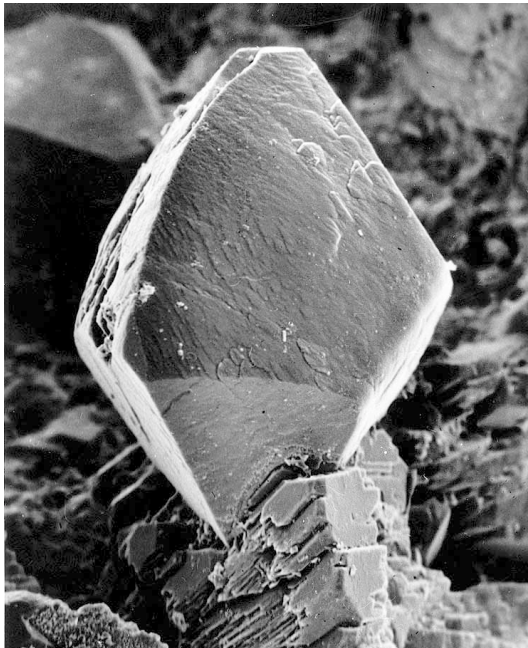


FIG. 3. Bipyramidal zoned crystal of ancylite-(Ce) - calcio-ancylite-(Ce) from a perovskite-titanite segregation in CAPR. Vertical dimension of the crystal: 850 μm .

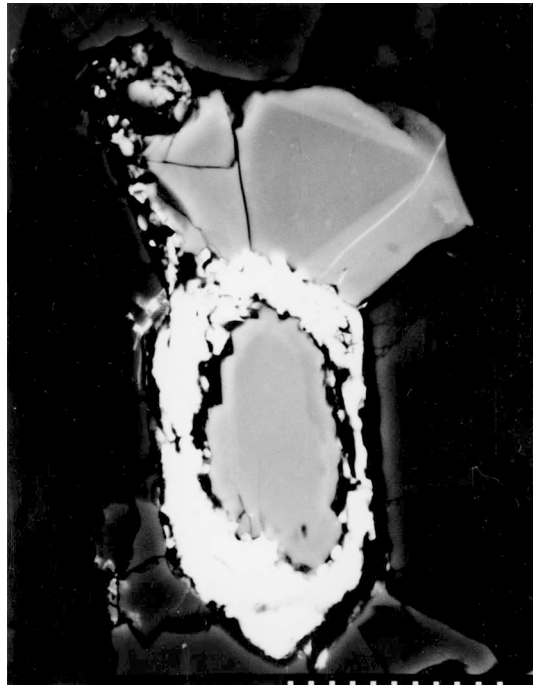


FIG. 4. Rim of ancylite-(Ce) (white) on hydroxylapatite (gray), black: calcite. Note the presence of weak zoning of the hydroxylapatite crystals. BSE image. Scale bar: 27 μm .

TABLE 2. REPRESENTATIVE COMPOSITIONS OF ANCYLITE-(Ce) AND CALCIO-ANCYLITE-(Ce) FROM AFRIKANDA (WT.%)

Point	1	2	3	4	5	6	7	8	9	10
Position	core			mantle		rim	core	mantle		rim
Mineral	Ancylite-(Ce)					Calcio-ancylite-(Ce)				
CaO	1.27	2.30	3.73	3.79	3.27	5.75	6.96	7.09	7.28	6.86
FeO	na	na	na	na	na	na	0.16	0.23	0.17	na
SrO	16.87	18.61	12.66	10.40	13.05	7.90	3.87	3.27	3.35	7.20
BaO	0.62	nd	0.18	0.78	1.01	2.37	0.13	nd	0.07	0.41
La ₂ O ₃	13.33	17.37	15.97	12.63	12.36	11.08	14.82	15.07	15.11	11.95
Ce ₂ O ₃	25.87	23.84	25.55	28.74	25.67	29.44	34.31	33.86	33.67	26.73
Pr ₂ O ₃	5.43	3.70	5.11	2.12	2.85	3.09	3.06	3.31	3.02	4.88
Nd ₂ O ₃	8.89	5.20	8.11	7.48	6.68	9.15	8.10	8.23	8.09	7.51
Sm ₂ O ₃	0.52	nd	nd	nd	nd	nd	nd	nd	0.18	nd
ThO ₂	nd	nd	nd	nd	0.13	nd	nd	0.12	nd	6.61
F	na	na	na	na	na	na	1.25	1.22	1.20	na
-O=F							0.53	0.51	0.50	
Total	72.80	71.02	71.31	65.94	65.02	68.78	72.13	71.89	71.64	72.15
	Formulae based on 2 CO ₃ ²⁻ and 1 (OH) ⁻ groups									
Ca	0.083	0.151	0.241	0.259	0.223	0.392	0.434	0.443	0.455	0.468
Fe							0.008	0.011	0.008	
Sr	0.597	0.662	0.443	0.384	0.482	0.292	0.131	0.111	0.113	0.266
Ba	0.015		0.004	0.019	0.025	0.059	0.003		0.002	0.010
La	0.300	0.393	0.356	0.297	0.290	0.260	0.318	0.324	0.325	0.281
Ce	0.578	0.535	0.564	0.670	0.598	0.686	0.731	0.722	0.718	0.623
Pr	0.121	0.083	0.112	0.049	0.066	0.072	0.065	0.070	0.064	0.113
Nd	0.194	0.114	0.175	0.170	0.152	0.208	0.169	0.171	0.168	0.171
Sm	0.011								0.004	
Th					0.002			0.002		0.096
Total	1.899	1.938	1.895	1.848	1.838	1.969	1.859	1.854	1.857	2.028
F							0.231	0.225	0.221	
REE	1.204	1.125	1.207	1.186	1.106	1.226	1.283	1.287	1.279	1.188
Sr/Ca	7.19	4.38	1.84	1.48	2.16	0.74	0.30	0.25	0.25	0.57

1-3 anhedral grains associated with low Sr calcite; 4-6 and 7-9 zoned euhedral crystals in cavities; 10 unzoned euhedral crystal; na = not analyzed; nd = not detected; total Fe expressed as FeO. Compositions 1-6 and 10 were obtained by EDS, and 7-9 by WDS.

in crystals with a strong intragranular zoning (Table 2, anal. 4-6).

The ancylite-(Ce) making up the rim on hydroxyl-apatite is, in some cases, intimately associated with britholite-(Ce) and an unidentified Sr-Ca-REE carbonate. The latter mineral contains high levels of REE (64.0-66.5 wt.% REE₂O₃), appreciable Ca and Sr (6.5-7.0 and 2.1-2.7 wt.% respective oxides), and relatively minor Ba (0.2-1.0 wt.% BaO). La is the dominant rare-earth element (29.6-31.8 wt.% La₂O₃), whereas Ce contents are systematically low (1.9-2.8 wt.% Ce₂O₃). The overall chemical composition may be expressed by the empirical formula (Ca,Sr)(La,REE)₃(CO₃)₄(OH)₃. This mineral most likely represents a member of the ancylite

family, *i.e.*, "calcio-ancylite-(La)", but at present, we are not able to make a confident identification.

In other carbonatite complexes, ancylite-(Ce) normally occurs in late-stage dolomite or ankerite carbonatites (*e.g.*, Kapustin 1980 and references therein, Bulakh *et al.* 1998). In some instances, it represents a product of late-stage alteration of primary REE-bearing minerals [*e.g.*, perovskite: Mitchell & Chakhmouradian (1998); burbankite: Zaitsev *et al.* (1998)]. Ancylite-(Ce) from carbonatites normally contains low to moderate levels of Ca (0.9-2.6 wt.% CaO: Bulakh *et al.* 1998, Zaitsev *et al.* 1998). Calcio-ancylite-(Ce) apparently is very rare in these rocks; to the best of our knowledge, it has been previously reported only from sulfide-rich

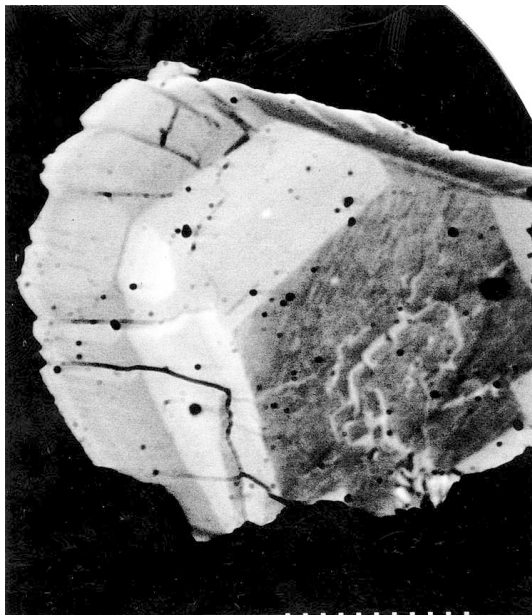


Fig. 5. Pattern of zoning in a crystal of ancylite-(Ce)–calcio-ancylite-(Ce), with ancylite-(Ce) in the core and calcio-ancylite-(Ce) in the rim. BSE image. Scale bar: 150 μm .

carbonatites associated with syenitic rocks of the Rocky Boy stock in Montana (Reguir & Mitchell 2000). Calcian ancylite-(Ce) (up to 4.5 wt.% CaO) and Sr-poor calcio-ancylite-(Ce) (0.2–2.6 wt.% SrO) occur in agpaitic alkaline parageneses at Narssárssuk and Ilímaussaq (Greenland) and Gordon Butte (Montana) (Pekov *et al.* 1997, Chakhmouradian & Mitchell 2001).

Strontianite

This is a rare mineral in CAPR, occurring intergrown with ancylite and barite and, less commonly, as platy crystals enclosed in calcite. The small size of these crystals (<7 μm) precluded accurate determination of their chemical composition. Our semiquantitative data suggest that the Afrikanda material contains appreciable Ca (2.1–3.7 wt.% of CaO) and minor Ba (0.1–0.6 wt.% BaO), typical substituent elements in strontianite from carbonatites (Kapustin 1980, Bulakh *et al.* 1998, Zaitsev *et al.* 1998).

Na-bearing carbonate minerals

These minerals are rare in CAPR; they are found exclusively as inclusions in the primary oxide minerals or hydroxylapatite. *Burbankite-group minerals* form minute (5–10 μm) round inclusions in REE–Nb-enriched perovskite, and abundant oval to round inclusions (1–20 μm across) in prismatic hydroxylapatite (Fig. 7).

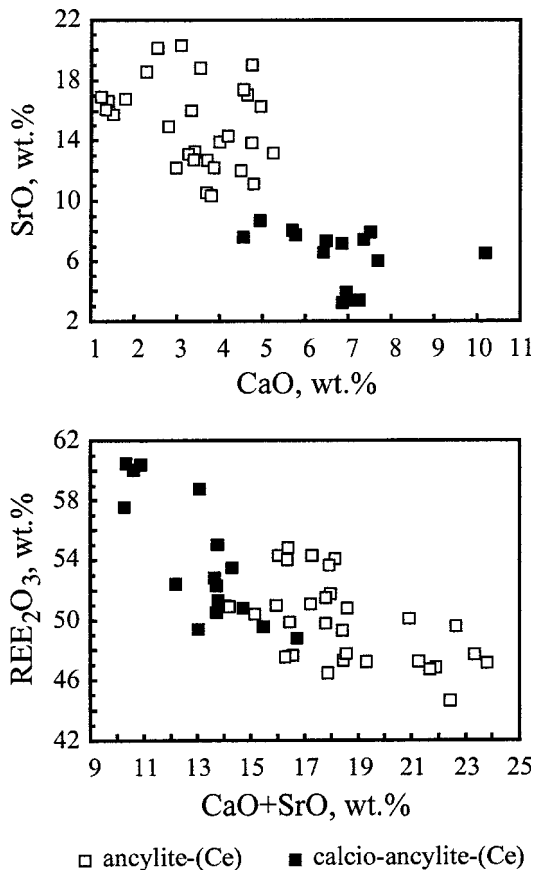


Fig. 6. Compositional variation (wt.%) of ancylite-(Ce) and calcio-ancylite-(Ce): (a) CaO versus SrO, and (b) CaO + SrO versus REE₂O₃.

The inclusions in hydroxylapatite are arranged in strings confined exclusively to the core of the crystals. On the basis of their chemical composition and Raman spectra, the minerals were classified as burbankite, (Na,Ca)₃(Sr,Ba,REE,Ca)₃(CO₃)₅, and its Ba-dominant analogue khanneshite (Table 3). No other elements were detected in the EDS spectra; the analytical total, including the CO₂ contents calculated from stoichiometry, ranges between 91 and 103 wt.%.

In common with burbankite and related minerals from other localities (Pekov *et al.* 1998, Zaitsev *et al.* 1998, Subbotin *et al.* 1999), burbankite and khanneshite from Afrikanda show a significant compositional variation, *i.e.*, 4.9–9.3 wt.% Na₂O, 7.2–10.2% CaO, 12.6–17.0% SrO, 10.3–24.5% BaO and 10.6–18.4% REE₂O₃. Low analytical totals in some of the analyses, as well as low cation totals, probably result from the loss of Na from the sample under the electron beam (*e.g.*, Platt & Woolley 1990). In secondary-electron images, the dam-

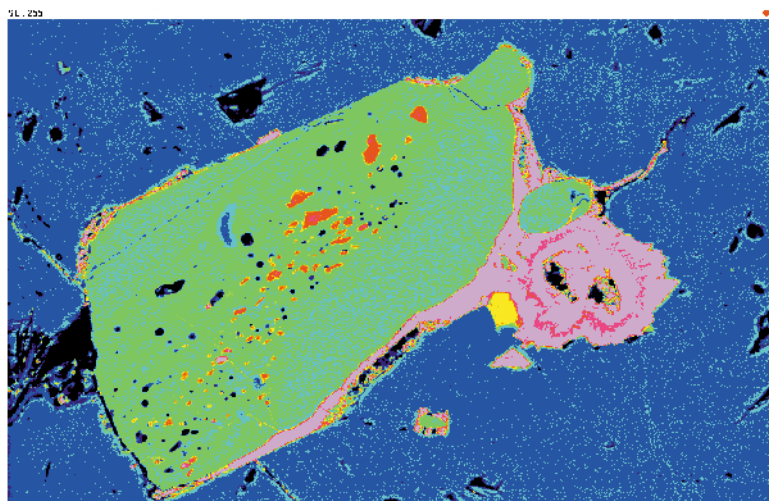


FIG. 7. Inclusions of khanneshite (red) in hydroxylapatite (green); the other minerals are ancyllite-(Ce) intergrown with cerite-(Ce) (mauve), calcite (blue) and perovskite (yellow). False-color BSE image. Note that the inclusions are confined to the core of a hydroxylapatite crystal.

TABLE 3. REPRESENTATIVE COMPOSITIONS OF BURBANKITE AND KHANNESHITE FROM AFRIKANDA (WT.%)

Point	1	2	3	4	5
Mineral	Burbankite		Khanneshite		
Na ₂ O	9.02	9.00	7.47	7.31	9.26
CaO	8.81	7.96	8.24	8.43	7.23
SrO	15.65	16.29	16.82	13.49	12.61
BaO	18.74	18.42	20.17	23.96	24.47
La ₂ O ₃	7.53	8.46	6.10	5.75	6.00
Ce ₂ O ₃	6.46	6.38	5.92	6.63	7.13
Pr ₂ O ₃	1.45	0.45	0.93	na	na
Nd ₂ O ₃	1.04	0.72	0.70	1.40	1.47
Total	68.70	67.68	66.35	66.97	68.17
	Formulae based on 5 (CO ₃) ²⁻ groups				
Na	2.003	2.042	1.756	1.732	2.155
Ca	0.653	0.634	0.820	0.825	0.602
Total	2.656	2.676	2.576	2.557	2.757
Sr	1.039	1.105	1.183	0.956	0.878
Ba	0.841	0.845	0.959	1.148	1.152
Ca	0.428	0.363	0.251	0.279	0.328
La	0.318	0.365	0.273	0.259	0.266
Ce	0.271	0.273	0.263	0.297	0.313
Pr	0.060	0.019	0.041		
Nd	0.043	0.030	0.030	0.061	0.063
Total	3.000	3.0000	3.000	3.000	3.000

1-5 inclusions in apatite. All compositions were obtained by EDS; na = not analyzed.

age is clearly visible on the surface of inclusions even after their short-term exposure to the beam.

The Na–Ca carbonate minerals *nyerereite* and *shortite* are rare in CAPR, found exclusively as inclusions in titaniferous magnetite and perovskite. In the magnetite, *nyerereite* occurs in association with calcite and hydroxylapatite in composite inclusions up to 30 × 70 μm in size, and alongside ilmenite lamellae (neither calcite nor hydroxylapatite is observed in this environment) (Fig. 8). In perovskite, *shortite* forms homogeneous round inclusions from 5 to 10 μm in diameter.

Accurate determination of the chemical composition of these inclusions was difficult because of their small size and low stability under the electron beam. The loss of Na probably explains systematically low analytical totals and deviations from stoichiometry. Element-distribution maps for the composite inclusion in magnetite and associated ilmenite show that the Na–Ca carbonate is uniform in composition (Fig. 8), although the observed difference in brightness may be partly attributed to surface heterogeneities. The inclusions in magnetite and perovskite differ in terms of their Na, Ca and K contents (Table 4, anal. 1–2 and 3–4, respectively). The *nyerereite* inclusions in magnetite are richer in Na (23.7–25.0 wt.% Na₂O) and poorer in Ca (26.1–27.1 wt.% CaO) than *shortite* inclusions in perovskite (12.2–16.5 wt.% Na₂O and 34.2–36.0 wt.% CaO). The latter also contain minor to moderate amounts of Ba, and minor K, Mn and Sr (<0.4 wt.% respective oxides). The relatively high levels of Fe detected in the *nyerereite*, calcite and hydroxylapatite may result from excitation of the magnetite host.

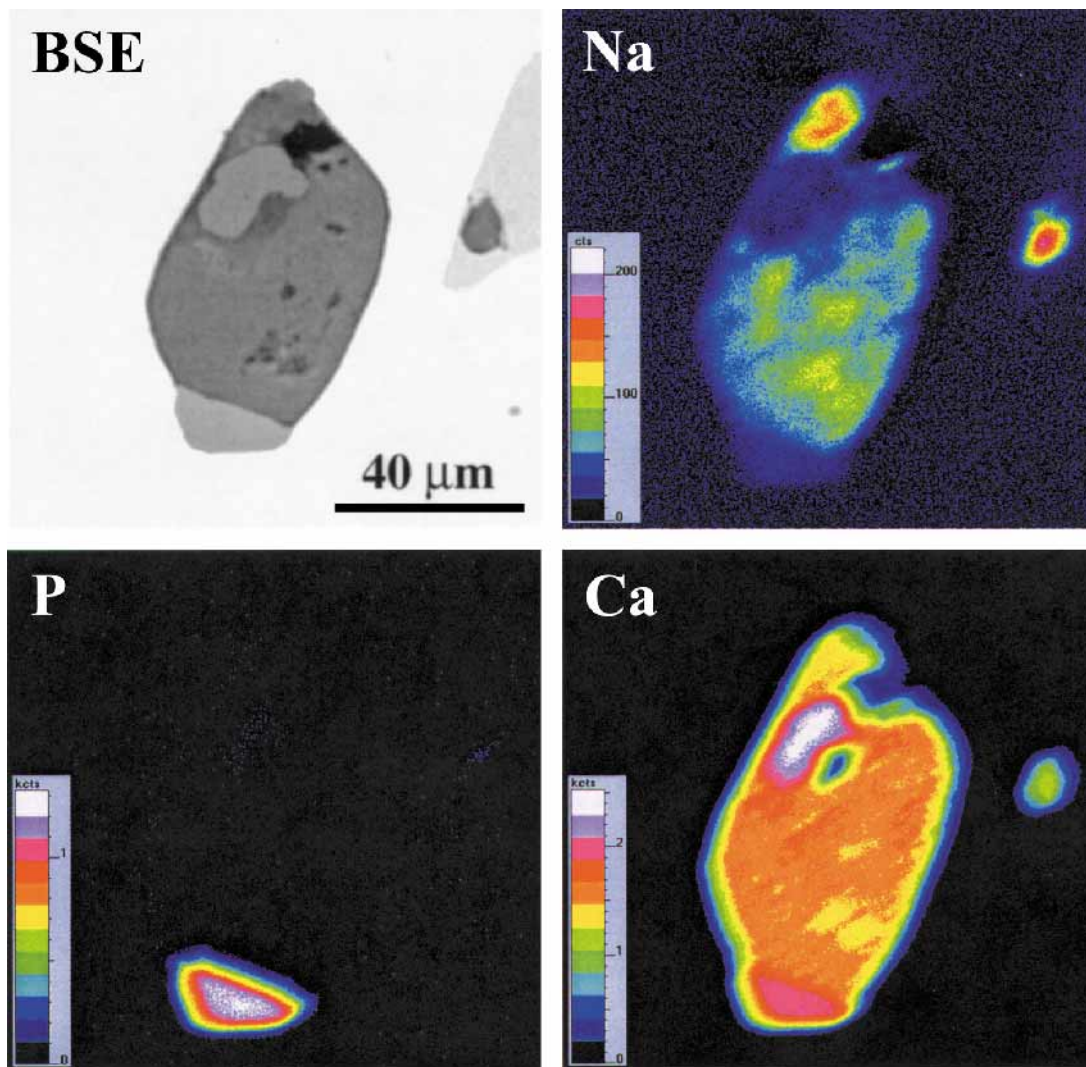


FIG. 8. BSE image and X-ray element-distribution maps of a composite calcite – nyerereite – apatite inclusion in magnetite.

On the $\text{Na}_2\text{CO}_3\text{--K}_2\text{CO}_3\text{--CaCO}_3$ diagram (Fig. 9), the compositions of inclusions in magnetite cluster near the ideal composition of nyerereite, $\text{Na}_2\text{Ca}(\text{CO}_3)_2$, whereas the perovskite-hosted inclusions plot near the shortite composition, $\text{Na}_2\text{Ca}_2(\text{CO}_3)_3$. Compositionally similar carbonate inclusions have been described in perovskite and calzirtite from calcite carbonatite of the Guli complex in Siberia (Kogarko *et al.* 1991) (Fig. 9). Some of the inclusions from Guli are significantly enriched in K (up to 3.9 wt.% K_2O), a feature that is not observed in the Afrikanda samples. Inclusions compositionally similar to K-enriched nyerereite and shortite (up to 5.5 wt.% K_2O) have been observed in forsterite, diopside, melilite and perovskite from ultramafic and

alkaline rocks of the Gardiner complex in Greenland, and in forsterite and clinopyroxene from ultramafic, alkaline and carbonatitic rocks of the Kovdor complex in Kola (Veksler *et al.* 1998).

The Na–Mg phosphate–carbonate *bradleyite* occurs as inclusions in discrete crystals of ilmenite. There are both numerous anhedral grains ranging from 1 to 15 μm in size and relatively large (20–50 μm) euhedral crystals present among the inclusions. BSE imaging and element-distribution maps show a uniform distribution of Na, Mg and P (Fig. 10). The chemical composition of the inclusions matches well the ideal formula of *bradleyite* if we assume the presence of CO_2 in the mineral (Table 4, anal. 5–6). Na–Mg–P minerals stochio-

TABLE 4. REPRESENTATIVE COMPOSITIONS OF NYEREREITE, SHORTITE AND BRADLEYITE FROM AFRIKANDA (WT.%)

Point	1	2	3	4	5	6
Mineral	Nyerereite		Shortite		Bradleyite	
Na ₂ O	24.81	23.72	16.45	16.02	34.28	33.75
MgO	na	na	na	na	14.75	14.03
K ₂ O	nd	nd	0.22	0.21	nd	nd
CaO	26.78	27.07	34.19	34.35	0.64	0.76
MnO	nd	0.05	0.12	0.13	0.48	0.57
FeO	0.81	0.67	1.71	1.72	1.12	1.38
SrO	0.07	0.16	0.22	0.21	na	na
BaO	nd	nd	3.02	nd	na	na
P ₂ O ₅	na	na	na	na	28.01	27.86
Total	52.47	51.67	55.93	52.64	79.28	78.35
Formulae based on:						
	2 CO ₃ ²⁻ groups		3 CO ₃ ²⁻ groups		5 cations	
Na	1.800	1.746	1.722	1.721	2.910	2.911
Mg					0.963	0.932
K			0.015	0.015		
Ca	1.073	1.101	1.978	2.039	0.030	0.036
Mn		0.002	0.005	0.006	0.018	0.021
Fe	0.025	0.021	0.077	0.080	0.041	0.051
Sr	0.002	0.004	0.007	0.007		
Ba			0.064			
P					1.038	1.049
Total	2.900	2.874	3.868	3.868	5.000	5.000
Na/Ca	1.68	1.59	0.87	0.84		

1-2 inclusions in magnetite; 3-4 inclusions in perovskite; 5-6 inclusions in ilmenite. na = not analyzed; nd = not detected; total Fe expressed as FeO. Compositions 1-4 were obtained by EDS, and 5-6 by WDS.

metrically similar to bradleyite have also been found as inclusions in forsterite from the Kovdor phoscorites and carbonatites (Veksler *et al.* 1998), in magnetite, lueshite and pyrochlore from the Sallanlatvi calcite carbonatites, and in lueshite from the Kovdor dolomite carbonatite (authors' unpubl. data).

Phosphate minerals

Hydroxylapatite is a common accessory mineral in CAPR. It occurs as euhedral (10–50 µm in diameter) or elongate, almost elliptical grains up to 200 µm in length. The crystals are typically enclosed in calcite and, less commonly, magnetite, perovskite and other rock-forming minerals. Rarely, hydroxylapatite is observed as slender prismatic and acicular crystals (up to 75 × 10 µm) arranged in radial aggregates and clumps up to 1 mm in diameter. Such aggregates are found predominantly in an assemblage with late-stage calcite and chlorite. Some prismatic crystals are replaced from the rim by *REE*-bearing carbonates, britholite-(Ce), or both. The hexagonal shape of hydroxylapatite crystals is invariably

preserved, suggesting that the replacement occurred after the precipitation of the surrounding calcite (Fig. 4).

The hydroxylapatite contains 0.4–3.0 wt.% *REE*₂O₃ and 0.4–1.2 wt.% SrO, plus minor proportions of Na, Fe and Si (<0.6 wt.% of the respective oxides) and traces of Mn (Table 5, anal. 1–3). None of the analyzed crystals contain detectable F or Cl; hence, we identify this mineral as hydroxylapatite. In terms of its Sr and *REE* contents, hydroxylapatite from Afrikanda is akin to apatite (*sensu lato*) from other Kola carbonatites and phoscorites (Rimskaya-Korsakova *et al.* 1979, Zaitsev *et al.* 1990, Arzamastseva *et al.* 1991). Generally speaking, low-to-moderate *REE* and Sr contents coupled with low Na and Si are characteristic of apatite-group minerals from carbonatitic rocks (Le Bas & Handley 1979, Egorov 1984, Hogarth 1989).

Britholite-(Ce) is a rare mineral in alkaline-carbonatite complexes (*e.g.*, Özgenç 2000). Among our samples, it was found only in two thin sections; in both cases, this mineral comprises replacement rims on the

TABLE 5. REPRESENTATIVE COMPOSITIONS OF PHOSPHATE MINERALS FROM AFRIKANDA (WT.%)

Point	1	2	3	4	5
Mineral	Hydroxylapatite		Britholite-(Ce)		
Na ₂ O	0.19	0.29	0.49	nd	nd
SiO ₂	0.52	nd	nd	15.68	16.38
P ₂ O ₅	39.82	42.38	40.79	8.91	8.62
CaO	52.23	53.29	53.63	20.02	19.76
FeO	nd	0.26	nd	nd	nd
MnO	nd	0.11	nd	nd	nd
SrO	1.09	1.02	0.63	0.63	0.53
La ₂ O ₃	0.42	nd	0.35	9.90	10.70
Ce ₂ O ₃	1.18	0.40	1.09	26.88	27.37
Pr ₂ O ₃	0.17	nd	nd	2.61	2.11
Nd ₂ O ₃	1.18	0.45	0.35	13.27	13.17
ThO ₂	nd	nd	nd	0.23	nd
Total	96.80	98.20	97.33	98.13	98.64
Formulae based on 12 O and 1 (OH) ⁻					
Si	0.045			1.942	2.014
P	2.932	3.021	2.964	0.934	0.897
Total	2.977	3.021	2.964	2.876	2.911
Ca	4.868	4.808	4.933	2.657	2.604
Na	0.032	0.047	0.082		
Fe		0.018			
Mn		0.008			
Sr	0.055	0.050	0.031	0.045	0.038
La	0.013		0.011	0.452	0.485
Ce	0.038	0.012	0.034	1.218	1.231
Pr	0.005			0.118	0.094
Nd	0.037	0.014	0.011	0.587	0.578
Th				0.006	
Total	5.048	4.957	5.102	5.083	5.030

nd = not detected; total Fe expressed as FeO. All compositions were obtained by EDS.

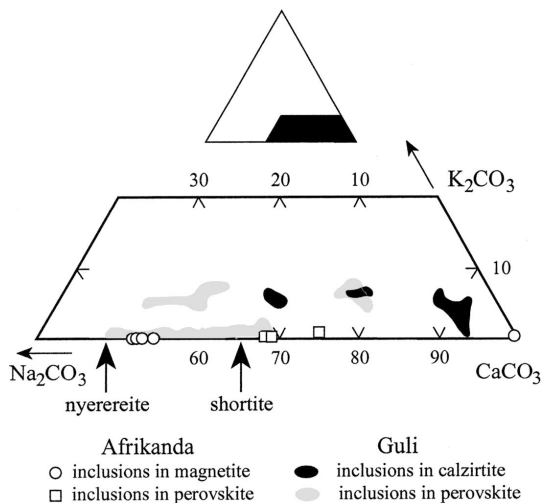


FIG. 9. Compositions of Na-Ca carbonate minerals in terms of the system $\text{Na}_2\text{CO}_3\text{-CaCO}_3\text{-K}_2\text{CO}_3$ (wt.%). Data for the Guli carbonatite are from Kogarko *et al.* (1991).

prismatic hydroxylapatite. In one of the samples, it is intimately associated with ancyllite-(Ce) and other REE minerals. The britholite contains between 51.8 and 54.2 wt.% REE_2O_3 , with Ce being the major lanthanide element (Table 5, anal. 4–5). The elevated P contents (8.1–9.3 wt.% P_2O_5) indicate the presence of about 30 mol.% $\text{Ca}_5(\text{PO}_4)_3(\text{OH})$ in our samples, arising from the substitution $\text{Ca}^{2+} + \text{P}^{5+} \leftrightarrow \text{REE}^{3+} + \text{Si}^{4+}$.

Barite

Barite is a ubiquitous late-stage mineral in carbonatites (*e.g.*, Kapustin 1980). In CAPR, this mineral occurs as scarce minute (<50 μm) inclusions in calcite, or as intergrowths with ancyllite-(Ce). The Afrikanda barite is unusual in containing high proportions of Sr (2.3–3.2 wt.% SrO) and Ca (0.9–2.5 wt.% CaO). Relatively high Sr contents have been previously reported by Kapustin (1980) for the “earlier colorless generation” of barite from some Kola carbonatites, and by Olson *et al.* (1954) for barite from the Mountain Pass carbonatites. It is noteworthy that the latter rocks are considered to be products of high-temperature magmatic crystallization. Late-stage and secondary barite is typically characterized by low Sr and Ca contents (Kapustin 1980, Wall & Mariano 1996, Bulakh *et al.* 1998, Zaitsev *et al.* 1998).

C–O ISOTOPE COMPOSITION OF CALCITE

Samples for C–O isotopic analyses were selected using CL observations from calcite crystals with the

minimal degree of secondary alteration. In total, five samples were hand-picked: one sample from paragenesis (1), two from a perovskite–titanite “nest”, and two from monomineralic calcite veins. The $\delta^{13}\text{C}$ and $\delta^{18}\text{O}$ values for these samples are presented in Table 6.

The data obtained show that calcite from different parageneses is characterized by similar isotopic composition of carbon ($\delta^{13}\text{C} = -2.5$ to -1.7‰ PDB), but shows a noticeable variation in $\delta^{18}\text{O}$ (9.3 to 12.1‰ SMOW). The lowest $\delta^{18}\text{O}$ value was obtained for calcite from paragenesis (1), whereas samples from paragenesis (2) and (3) gave comparatively higher $\delta^{18}\text{O}$ values. On the $\delta^{13}\text{C}$ – $\delta^{18}\text{O}$ diagram, the Afrikanda compositions form an elliptical field subparallel to the $\delta^{18}\text{O}$ axis (Fig. 11). In Figure 11, the isotopic data for other Kola carbonatites (Zaitsev & Bell 1995, Dunworth & Bell 2001, Zaitsev *et al.* 2001) and the Oldoinyo Lengai natrocarbonatite (Keller & Hoefs 1995) are plotted for comparison. Also shown is the so-called “carbonatite box” believed to represent the primary isotopic composition of carbonatites and of their hypothetical source in the mantle (Taylor *et al.* 1967, Hoefs 1987).

DISCUSSION

Do carbonatites exist at Afrikanda?

The calcite – amphibole – clinopyroxene rock is not a *bona fide* carbonatite, as it generally contains less than 15 vol.% of calcite; following the IUGS guidelines, it should be classified as calcite–amphibole clinopyroxenite. The petrographic observations suggest that the early calcite is the latest rock-forming mineral to crystallize, and that it formed in equilibrium with the silicate minerals. The available cathodoluminescence data show that this calcite is relatively homogeneous and has a simple pattern of zoning, indicating stable conditions of crystallization (Fig. 2a). High Sr contents in the early calcite (up to 1.4 wt.% SrO) are comparable with those in magmatic calcite from alkaline rocks (*e.g.*, calcite ijolites from Dicker Willem, Namibia: Cooper & Reid 1998), and early-stage carbonatites (Pouliot 1970, Sokolov 1985, Clarke *et al.* 1992, Dawson *et al.* 1996). Locally, the calcite – amphibole – clinopyroxene rocks are enriched in perovskite and titanite (up to 70 and 40 vol.%, respectively). These segregations are also enriched in calcite (up to 50 vol.%). The available petrographic and CL data indicate non-equilibrium between the oxide and silicate minerals, as well as partial dissolution of primary calcite, followed by its overgrowth with late-stage low-Sr calcite (Figs. 2b, c).

Carbonatite veins up to 5 cm in width were described by Kukharenko *et al.* (1965) from the fenite aureole of the Afrikanda complex, although carbonatite bodies have not been reported to occur within the pluton. In this work, we found several veins up to 20 cm wide cutting silicate rocks, as well as scattered blocks of coarse-grained calcite. The latter were not observed in

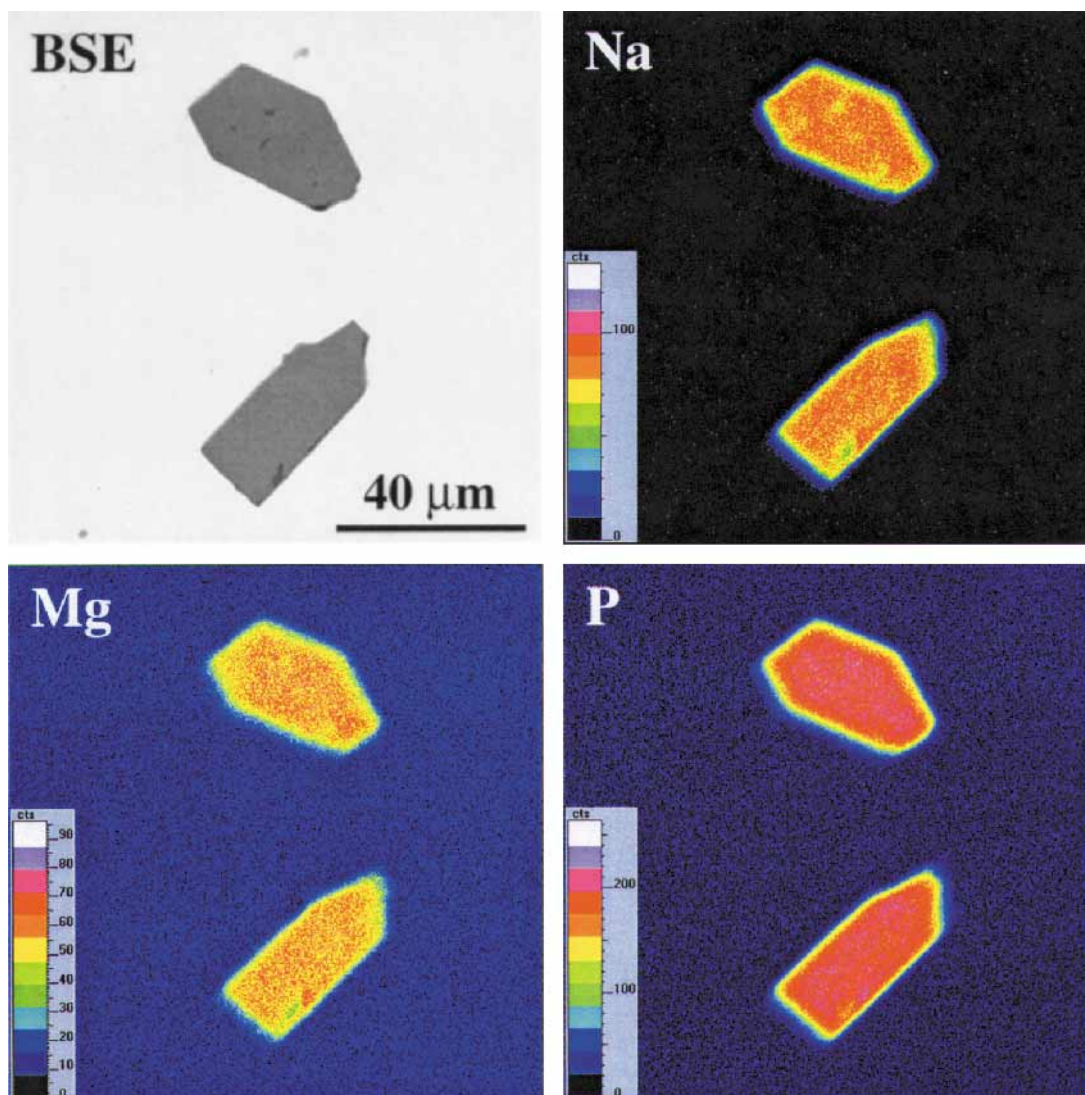


FIG. 10. BSE image and X-ray element-distribution maps of euhedral crystals of bradleyite enclosed in discrete crystals of ilmenite.

an outcrop, but their size (<50 cm across) and the scarcity of silicate minerals in these blocks suggest that their source veins (dikes ?) probably exceeded 1 m in thickness. The mineralogy and geochemistry of the calcite veins and blocks are consistent with their identification as calcite carbonatites. The mineralogical evidence includes the modal composition of these rocks (major calcite with subordinate perovskite, magnetite and titanite) and the assemblage of accessory minerals characteristic of carbonatites (hydroxylapatite, ilmenite, ancyllite, calcio-ancyllite, barite, Ca–Zr–Ti oxides,

pyrochlore and zircon). Compositionally, the minerals from Afrikanda (*e.g.*, Sr-enriched calcite, barite and hydroxylapatite) are similar to their counterparts in other Kola carbonatites (*e.g.*, Khibina, Vuoriyarvi and Sallanlatvi: Kapustin 1980, Zaitsev *et al.* 1990, Zaitsev 1996, Sitnikova *et al.* 2000).

Rare-earth mineralization

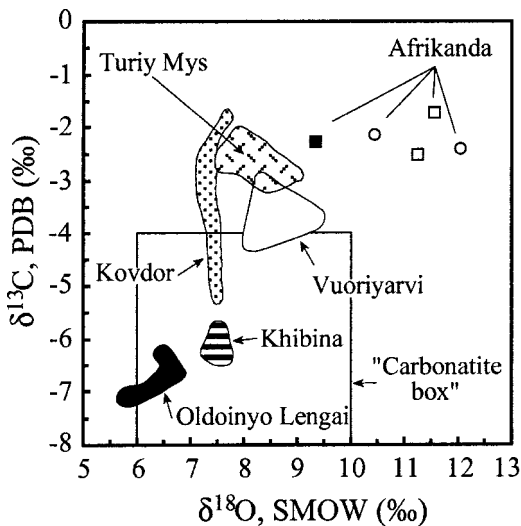
The presence of REE minerals, *i.e.*, of the burbankite – khanneshite and ancyllite – calcio-ancyllite-(Ce) series,

TABLE 6. CARBON AND OXYGEN ISOTOPIC COMPOSITION OF CALCITE FROM AFRIKANDA

Sample	Paragenesis	$\delta^{13}\text{C}$ ‰ PDB	$\delta^{18}\text{O}$ ‰ SMOW
AFR 11	1	-2.3	9.3
AFR 9	2	-1.7	11.6
AFR 13	2	-2.5	11.2
AFR 1	3	-2.1	10.4
AFR 10	3	-2.4	12.1

also supports a close affinity between CAPR and carbonatitic rocks elsewhere in the Kola Alkaline Province. Burbankite and ancylite-(Ce) are characteristic accessory minerals in many of the Kola carbonatites; both minerals have been described from Vuoriyarvi and Khibina (Kukhareno *et al.* 1965, Kapustin 1980, Zaitsev *et al.* 1998), whereas ancylite-(Ce) is also common at Sallanlatvi and Seblyavr (Orlova *et al.* 1963, Bulakh *et al.* 1998). Where the two minerals occur in the same carbonatite, burbankite invariably precedes ancylite-(Ce), and in some cases, becomes replaced by that mineral. At Afrikanda, burbankite and khanneshite form inclusions in the early-crystallized minerals (perovskite and hydroxylapatite), whereas ancylite-(Ce) and calcio-ancylite-(Ce) are associated with veinlets and patches of low-Sr calcite, or occur as late-stage euhedral crystals in cavities. These morphological features clearly indicate the early crystallization of burbankite–khanneshite relative to ancylite-group phases.

The ratio $\text{La}/\text{Nd}_{\text{CN}}$ in REE minerals is a useful indicator of paragenetic type and environment of crystallization (Fleischer 1965, 1978, Fleischer & Altschuler 1969). In the burbankite–khanneshite series, values are highly variable, ranging from 7.6–7.7 for khanneshite to 10.7–22.8 for burbankite. In contrast, $\text{La}/\text{Nd}_{\text{CN}}$ in ancylite-(Ce) and calcio-ancylite-(Ce) is low and ranges from 2.1 to 3.7, and from 1.7 to 3.8, respectively. In a detailed study of the REE minerals from the Khibina complex, Zaitsev *et al.* (1998) demonstrated that $\text{La}/\text{Nd}_{\text{CN}}$ in these minerals decreases in the same order as the relative age of rocks: calcite carbonatite → ankerite carbonatite → siderite–rhodochrosite carbonatites → hydrothermal carbonate–zeolite rocks. The observed decrease was interpreted to reflect a gradual increase in the proportion of a “carbohydrothermal” fluid in the carbonatite-forming system. The $\text{La}/\text{Nd}_{\text{CN}}$ values of the Afrikanda burbankite and khanneshite are similar to or higher than those of the Khibina burbankite, which is now interpreted as having formed from a volatile-rich carbonatitic melt (Wall *et al.* 2000). The $\text{La}/\text{Nd}_{\text{CN}}$ values for ancylite-(Ce) and calcio-ancylite-(Ce) are close to those for the REE minerals from the late-stage siderite–rhodochrosite carbonatites and carbonate–zeolite hydrothermal rocks at Khibina, and thus are consistent with crystallization of the ancylite-group minerals from Afrikanda under low-temperature hydrothermal conditions.



- calcite-amphibole-clinopyroxene rock
- calcite-perovskite-titanite segregation in CAPR
- monomineralic calcite rock

FIG. 11. Isotopic compositions of carbon and oxygen in calcite. Shown for comparison are the data for Khibina and Vuoriyarvi (Zaitsev *et al.* 2001), Kovdor (Zaitsev & Bell 1995), Turiy Mys (Dunworth & Bell 2001), Oldoinyo Lengai (Keller & Hoefs 1995), and the so-called “carbonatite box” (Taylor *et al.* 1967, Hoefs 1987).

ite–rhodochrosite carbonatites and carbonate–zeolite hydrothermal rocks at Khibina, and thus are consistent with crystallization of the ancylite-group minerals from Afrikanda under low-temperature hydrothermal conditions.

Inclusions of Na-carbonate

Na-, K-, Ca- and Mg-rich carbonate inclusions that are inferred to have crystallized from melt occur in carbonatite minerals from the Guli and Kovdor complexes (Kogarko *et al.* 1991, Veksler *et al.* 1998). Na–Ca-rich inclusions also have been reported from phoscorites and associated silicate rocks (olivinite, peridotite, clinopyroxenite and melilitolite) of the Gardiner and Kovdor plutons (Nielsen *et al.* 1997, Veksler *et al.* 1998). Their appearance was interpreted to result from late-stage alkali enrichment in a parental carbonatite-forming system.

In terms of the mineral assemblages, the inclusions in CAPR are more similar to those from the Guli carbonatites than to those from Kovdor or Gardiner. Perovskite and calzirtite from Guli contain inclusions of carbonate phases only, whereas at Kovdor and Gardiner, the Na–Ca-rich phases are associated with

silicate minerals such as phlogopite, amphibole and clinopyroxene. In CAPR, the Na–Ca-rich inclusions hosted by magnetite and perovskite were identified as nyerereite and shortite, respectively. As magnetite precipitated earlier than perovskite (Chakhmouradian & Zaitsev 1999), we infer that the carbonatite system evolved by becoming depleted in Na and enriched in Ca. The early crystallization of the nyerereite–calcite assemblage (Fig. 8) relative to shortite is supported by phase relationships in the system $\text{Na}_2\text{CO}_3\text{–CaCO}_3$ (Cooper *et al.* 1975). In that system, shortite is stable up to 400°C ($P = 1$ kbar), and the association of nyerereite + calcite is observed between 400 and 817°C ($P = 1$ kbar). The latter range in temperature agrees well with the estimate of Chakhmouradian & Zaitsev (1999) that the Afrikanda magnetite crystallized above 550°C. The relationship between nyerereite and shortite can be expressed by the equilibrium $\text{Na}_2\text{Ca}(\text{CO}_3)_2 + \text{CaCO}_3 \leftrightarrow \text{Na}_2\text{Ca}_2(\text{CO}_3)_3$; however, the inadequacy of thermodynamic data for the Na carbonate phases does not allow calculation of the range of their P – T stability.

Low Sr contents (<0.15 wt.% SrO) in calcite associated with nyerereite (Fig. 8) seem paradoxical; it is reasonable to expect that high-temperature calcite should be rich in Sr. In contrast, hydroxylapatite from the same association is rich in Sr (0.9–1.1 wt.% SrO). The equilibrium coexistence of low-Sr calcite with Sr-enriched hydroxylapatite contradicts the observations previously made that the $K_D(\text{Sr})$ values for the pair calcite–apatite are always greater than unity (Zaitsev & Bell 1995, Dawson *et al.* 1996). At present, it is not clear whether the observed distribution of Sr between hydroxylapatite and calcite reflects specific conditions of crystallization in an alkali-rich carbonatitic system, or simply results from the early sequestration of Sr in hydroxylapatite prior to the precipitation of the carbonates.

Variations in the carbon and oxygen isotopes

Recent studies of the C–O isotopic composition of carbonate minerals from phoscorites and carbonatites of the Kovdor, Khibina, Turiy Mys and Vuoriyarvi complexes (Fig. 11) have demonstrated that there is a significant variation in the isotopic composition of C, and relatively little variation in the isotopic composition of O (Zaitsev & Bell 1995, Dunworth & Bell 2001, Zaitsev *et al.* 2001). It is noteworthy that altered samples and those inferred to be contaminated with a crustal component are not shown on Figure 11. For the majority of samples from these localities, $\delta^{18}\text{O}$ values are between 7.2 and 8.6‰ SMOW, with a few samples showing elevated $\delta^{18}\text{O}$ values, between 9.0 and 9.4‰ SMOW. The $\delta^{13}\text{C}$ values vary from one carbonatite to the other. The Khibina carbonatites have the most “primitive” C isotopic signature ($\delta^{13}\text{C}$ in the range –6.4 to –5.8‰ PDB) in comparison with other phoscorites and carbonatites. Calcite from the Turiy Mys phoscorites and carbonatites is characterized by $\delta^{13}\text{C}$ values in the range from –3.1

to –2.1‰ PDB. Calcite from the Vuoriyarvi carbonatites, as well as from the Kovdor phoscorites and carbonatites, has an isotopic composition intermediate between that of Khibina and Turiy Mys ($\delta^{13}\text{C}$ from –5.2 to –2.6‰ and from –4.2 to –3.0‰ PDB for the Kovdor and Vuoriyarvi samples, respectively). Among all samples, dolomite from the Kovdor carbonatites has the highest $\delta^{13}\text{C}$ value, –1.8‰ PDB.

Variations in the isotopic composition of C in the Afrikanda calcite ($\delta^{13}\text{C}$ from –2.5 to –1.7‰) are similar to those observed in calcite from Turiy Mys and Kovdor, and dolomite from Kovdor. In contrast, the oxygen isotopic values are generally higher in the Afrikanda samples relative to the other localities. Only the calcite sample from paragenesis (1) has a $\delta^{18}\text{O}$ value comparable to that for the Vuoriyarvi dolomite. As our CL observations document very little alteration in this calcite, or none at all, we consider the $\delta^{13}\text{C}$ and $\delta^{18}\text{O}$ values obtained (–2.3 and 9.3‰, respectively) as the most “primitive” for the Afrikanda rocks. Calcite from parageneses (2) and (3) (perovskite–titanite segregation and carbonatites, respectively) have similar $\delta^{13}\text{C}$ values, but show large variations in $\delta^{18}\text{O}$. These variations cannot be interpreted as a result of protracted Rayleigh fractionation during the formation of CAPR and carbonatite, because such a process should produce enrichment of both ^{13}C and ^{18}O . It is more likely that the $\delta^{18}\text{O}$ values, between 10.4 and 12.1‰, coupled with the fairly uniform isotopic composition of C, result from alteration of calcite in parageneses (2) and (3). The available CL data showing internal heterogeneity of calcite (embayed contacts between the zones, cross-cutting veinlets, irregular patches within the crystals), as well as the occurrence of Sr-poor calcite and ancylite along fractures, strongly suggest that the initial isotopic composition of calcite may have been affected by hydrothermal processes. On the basis of quantitative isotope-exchange models for the system $\text{CO}_2\text{–H}_2\text{O–CaCO}_3$ (Deines 1989, Santos & Clayton 1995, Ray & Ramesh 1999), the observed ^{18}O values can be explained in terms of reaction between calcite and a low-temperature (200–250°C) meteoric-hydrothermal fluid with a low $\text{CO}_2\text{:H}_2\text{O}$ ratio.

Possible reasons for the heterogeneous carbon isotopic composition and relatively invariant “primitive” $\delta^{18}\text{O}$ values in the Kola carbonatitic rocks have been previously discussed by Zaitsev & Bell (1995), Dunworth & Bell (2001), and Zaitsev *et al.* (2001). These authors proposed that the high $\delta^{13}\text{C}$ values could arise from: (i) isotopic re-equilibration of carbonates with Devonian seawater, (ii) contribution from an oxidized mantle carbon (either diamond or graphite) followed by formation of a carbonate melt, or (iii) mantle heterogeneity involving mixing of two components (Zaitsev & Bell 1995, Dunworth & Bell 2001). Alternatively, the high $\delta^{13}\text{C}$ values may be related to a crustal component, with the associated low $\delta^{18}\text{O}$ values indicating that the contamination occurred at high T in the

presence of a silicate melt (Zaitsev *et al.* 2001). This model implies that the mantle source was contaminated with subducted carbonate material, causing the enrichment in ^{13}C , whereas the oxygen isotopic composition was effectively buffered by the silicate melt. It is possible that both factor (ii) and subduction-related contamination are responsible for the $\delta^{13}\text{C}$ values observed in the Afrikanda samples. However, the proportion of heavy carbon contributed by each of these sources is uncertain.

CONCLUSIONS

Petrographic, mineralogical and geochemical data from this study and the previous work (Chakhmouradian & Zaitsev 1999) suggest that: (i) carbonatites are present in the Afrikanda complex, (ii) the early calcite in CAPR is a primary magmatic phase, as originally proposed by Kupletskii (1938), and (iii) CAPR and *bona fide* carbonatite are genetically related.

The presence of Na-bearing carbonate inclusions (and lueshite, NaNbO_3) in the early-crystallized minerals from CAPR (magnetite, perovskite, hydroxylapatite and ilmenite) indicates initially high activities of Na in the system. The subsequent evolution of the carbonatite system involved a decrease in $a(\text{Na}^{1+})$ accompanied by an increase in $a(\text{Ca}^{2+})$, as documented by the transition from nyerereite to shortite. The successive precipitation of baddeleyite, calzirtite and zirconolite also indicates a steady increase in $a(\text{Ca}^{2+})$ (Chakhmouradian & Zaitsev 1999).

Crystallization of ancyllite-(Ce) and calcio-ancyllite-(Ce) is related to low-temperature hydrothermal processes. Some of the *REE* and Sr required for the formation of these minerals was derived from dissolution of the primary perovskite and Sr-enriched calcite, as indicated by the occurrence of ancyllite (*sensu lato*) within veinlets and patches of low-Sr calcite and along fractures in perovskite.

Low-temperature (200–250°C) hydrothermal processes in the Afrikanda carbonatitic rocks were accompanied by isotope exchange between the primary calcite and a late-stage hydrothermal fluid. The isotopic composition of C in the Afrikanda calcite is characterized by elevated values of $\delta^{13}\text{C}$ analogous to those for the Turiy Mys and Kovdor phoscorites and carbonatites. The observed high $\delta^{13}\text{C}$ values in the carbonatites may reflect heterogeneity of the mantle beneath the Kola Craton (probably associated with a subduction-related contamination source: Zaitsev *et al.* 2001) and, possibly, contribution from the oxidation of mantle carbon (diamond or graphite) (Dunworth & Bell 2001).

ACKNOWLEDGEMENTS

We are grateful to D. Nattland (Institute of Physical Chemistry, Karlsruhe University) for help with Raman spectroscopic studies, J. Keller and D. Wiedenmann (In-

stitute of Mineralogy, Freiburg University) for help with CL microscopy, A. Danilewsky (Institute of Crystallography, Freiburg University) and V.N. Yakovenchuk (Geological Institute, Kola Science Center) for help with scanning electron microscopy, C.T. Williams and F. Wall (Department of Mineralogy, The Natural History Museum) for help with WDS electron-microprobe analyses, and K. Bell (Department of Earth Sciences, Carleton University) for access to the Stable Isotope Laboratory at the University of Ottawa. R.H. Mitchell and A.J. MacKenzie are thanked for allowing access to the scanning electron microscope at Lakehead University. We also thank The Natural History Museum, V.N. Yakovenchuk and A.V. Voloshin (Geological Institute, Kola Science Center) for providing the reference samples for our Raman-spectroscopic studies. The comments of G. Ferraris, I.V. Pekov and R.F. Martin helped to improve this paper. A.N. Zaitsev gratefully acknowledges the financial support from Alexander von Humboldt-Stiftung (including Europe Research Fellowship) and INTAS (project 97–0722 on the mineralogy and geochemistry of the Kola phoscorites and carbonatites).

REFERENCES

- ARZAMASTSEVA, L.V., BALAGANSKAYA, E.G., PAVLOV, V.P., PRIPACHKIN, V.A. & SHPACHENKO, A.K. (1991): New data on Khibina apatite deposits. *In* Apatite Content in Alkaline Massifs of the Kola Peninsula (O.B. Dudkin, ed.). Kola Science Center, Russian Academy of Sciences, Apatity, Russia (47–67; in Russ.).
- BUCKLEY, H.A. & WOOLLEY, A.R. (1990): Carbonates of the magnesite–siderite series from four carbonatite complexes. *Mineral. Mag.* **54**, 413–418.
- BÜHN, B., RANKIN, A.H., RADTKE, M., HALLER, M. & KNÖCHELL, A. (1999): Burbankite, a (Sr,REE,Na,Ca)-carbonate in fluid inclusions from carbonatite-derived fluids: identification and characterization using laser Raman spectroscopy, SEM–EDX, and synchrotron micro-XRF analysis. *Am. Mineral.* **84**, 1117–1125.
- BULAKH, A.G., LE BAS, M.J., WALL, F. & ZAITSEV, A.N. (1998): Ancyllite-bearing carbonatites of the Sebylavr massif, Kola Peninsula, Russia. *Neues Jahrb. Mineral., Monatsh.*, 171–192.
- BURKE, E.A.J. (2001): Raman microspectrometry of fluid inclusions. *Lithos* **55**, 139–158.
- CHAKHMOURADIAN, A.R. & MITCHELL, R.H. (2001): The mineralogy of Ba- and Zr-rich alkaline pegmatites from Gordon Butte, Crazy Mountains (Montana, USA): comparisons between potassic and sodic apatitic pegmatites. *Contrib. Mineral. Petrol.* (in press).
- _____ & ZAITSEV, A.N. (1999): Calcite – amphibole – clinopyroxene rock from the Afrikanda complex, Kola peninsula, Russia: mineralogy and a possible link to carbonatites. I. Oxide minerals. *Can. Mineral.* **37**, 177–198.

- CHIN TKHI LE TKHY, NADEZHINA, T.N., POBEDIMSKAYA, YE.A. & KHOMYAKOV, A.P. (1984): The crystal-chemical characteristics of bradleyite, sidorenkite and bonshtedtite. *Mineral. Zh.* **6**(5), 79-84 (in Russ.).
- CLARKE, L.B., LE BAS, M.J. & SPIRO, B. (1992): Rare earth, trace element and stable isotope fractionation of carbonatites at Kruidfontein, Transvaal, S. Africa. *In Proc. 5th Kimberlite Conf. 1. Kimberlite, Related Rocks and Mantle Xenoliths. CPRM, Spec. Publ.* **1**, 236-251.
- COOPER, A.F., GITTINS, J. & TUTTLE, O.F. (1975): The system $\text{Na}_2\text{CO}_3\text{--K}_2\text{CO}_3\text{--CaCO}_3$ at 1 kilobar and its significance in carbonatite petrogenesis. *Am. J. Sci.* **275**, 534-560.
- _____ & REID, D.L. (1998): Nepheline sövites as parental magmas in carbonatite complexes: evidence from Dicker Willem, southwest Namibia. *J. Petrol.* **39**, 2123-2136.
- DAWSON, J.B., STEELE, I.M., SMITH, J.V. & RIVERS, M.L. (1996): Minor and trace element chemistry of carbonates, apatites and magnetites in some African carbonatites. *Mineral. Mag.* **60**, 415-425.
- DEINES, P. (1989): Stable isotope variations in carbonatites. *In Carbonatites: Genesis and Evolution* (K. Bell., ed.). Unwin Hyman, London, U.K. (301-359).
- DUNWORTH, E.A. & BELL, K. (2001): The Turiy massif, Kola Peninsula, Russia: isotopic and geochemical evidence for multi-source evolution. *J. Petrol.* **42**, 377-405.
- EGOROV, L.S. (1984): Rare-earth element and fluorine contents of apatite as reflecting formation conditions, alteration, and potential mineralization for rocks of the phoscorite – carbonatite group in ijolite – carbonatite complexes. *Geochem. Int.* **21**(1), 93-107.
- FLEISCHER, M. (1965): Some aspects of the geochemistry of yttrium and the lanthanides. *Geochim. Cosmochim. Acta* **29**, 755-772.
- _____ (1978): Relative proportions of the lanthanides in minerals of the bastnaesite group. *Can. Mineral.* **16**, 361-363.
- _____ & ALTSCHULER, Z.S. (1969): The relationship of rare-earth composition of minerals to geological environment. *Geochim. Cosmochim. Acta* **33**, 725-732.
- FRIEDMAN, I. & O'NEIL, J.R. (1977): Compilation of stable isotope fractionation factors of geochemical interest. *In Data of Geochemistry* (M. Fleischer, ed.). *U.S. Geol. Surv., Prof. Pap.* **440-KK**.
- HOEFS, J. (1987): *Stable Isotope Geochemistry*. Springer, Berlin, Germany.
- HOGARTH, D.D. (1989): Pyrochlore, apatite and amphibole: distinctive minerals in carbonatites. *In Carbonatites: Genesis and Evolution* (K. Bell, ed.). Unwin Hyman, London, U.K. (105-148).
- KAPUSTIN, YU.L. (1980): *Mineralogy of Carbonatites*. Amerind Publishing Co, New Delhi, India.
- KELLER, J. & HOEFS, J. (1995): Stable isotope characteristics of recent natrocarbonatites from Oldoinyo Lengai. *In Carbonatite Volcanism: Oldoinyo Lengai and the Petrogenesis of Natrocarbonatites* (K. Bell & J. Keller, eds.). IAVCEI Proceedings in Volcanology. Springer, Berlin, Germany (113-123).
- KOGARKO, L.N., PLANT, D.A., HENDERSON, C.M.B. & KJARSGAARD, B.A. (1991): Na-rich carbonate inclusions in perovskite and calzirtite from the Guli intrusive Carbonatite, Polar Siberia. *Contrib. Mineral. Petrol.* **109**, 124-129.
- KUKHARENKO, A.A., ORLOVA, M.P., BULAKH, A.G., BAGDASAROV, E.A., RIMSKAYA-KORSAKOVA, O.M., NEFEDOV, E.I., ILINSKII, G.A., SERGEEV, A.S. & ABAKUMOVA, N.B. (1965): *The Caledonian Complex of Ultrabasic Alkaline Rocks and Carbonatites of the Kola Peninsula and Northern Karelia*. Nedra, Leningrad, Russia (in Russ.).
- KUPLETSKII, B.M. (1938): The pyroxenite intrusion near Afrikanda railway station in the Kola Peninsula. *Trudy Petrograph. Instit. Akad. Nauk SSSR* **12**, 71-88 (in Russ.).
- LE BAS, M.J. & HANDLEY, C.D. (1979): Variations in apatite composition in ijolitic and carbonatitic igneous rocks. *Nature* **279**, 54-56.
- MCCREA, J.M. (1950): On the isotopic chemistry of carbonates and a paleotemperature scale. *J. Chem. Phys.* **18**, 849-857.
- MITCHELL, R.H. & CHAKHMOURADIAN, A.R. (1998): Instability of perovskite in a CO_2 -rich environment: examples from carbonatite and kimberlite. *Can. Mineral.* **36**, 939-952.
- NIELSEN, T.F.D., SOLOVOVA, I.P. & VEKSLER, I.V. (1997): Parental melts of melilitolite and origin of alkaline carbonatite: evidence from crystallized melt inclusions, Gardiner complex. *Contrib. Mineral. Petrol.* **126**, 331-344.
- OLSON, J.C., SHAW, D.R., PRAY, L.C. & SHARP, W.N. (1954): Rare-earth mineral deposit of the Mountain Pass district, San Bernardino County, California. *U.S. Geol. Surv., Prof. Pap.* **261**.
- ORLOVA, M.P., ROZHDESTVENSKIY, YU.P. & BARANOVA, E.N. (1963): On the mineralogy of rare-metal carbonatites of the Sallanlatvi massif (northern Karelia). *Trudy VSEGEI, Novaya Seriya* **96**, 3-20 (in Russ.).
- ÖZGENÇ, I. (2000): Characteristics of Turkish carbonatites. *In Carbonatites 2000: Genèse et Minéralisations Associées*, Abstracts, 36.
- PEKOV, I.V., CHUKANOV, N.V. & BELOVITSKAYA, YU.V. (1998): Khanneshite and petersenite-(Ce) from the Khibina massif. *Zap. Vser. Mineral. Obshchest.* **127**(2), 92-100 (in Russ.).
- _____, PETERSEN, O.V. & VOLOSHIN, A.V. (1997): Calcio-ancylite-(Ce) from Ilímaussaq and Narssarsuk, Greenland, Kola Peninsula and Polar Urals, Russia: ancylite-(Ce) – calcio-ancylite-(Ce) an isomorphous series. *Neues Jahrb. Mineral., Abh.* **171**, 309-322.

- PLATT, R.G. & WOOLLEY, A.R. (1990): The carbonatites and fenites of Chipman Lake, Ontario. *Can. Mineral.* **28**, 241-250.
- POULIOT, G. (1970): Study of carbonatitic calcites from Oka, Quebec. *Can. Mineral.* **10**, 511-540.
- RAY, J.S. & RAMESH, R. (1999): Evolution of carbonatite complexes of the Deccan flood basalt province: stable carbon and oxygen isotopic constrains. *J. Geophys. Research* **104**, 29471-29483.
- REGUIR, E.P. & MITCHELL, R.H. (2000): The mineralogy of carbonatites and related potassic syenites from the Rocky Boy stock, Bearpaw Mountains, north-central Montana. *Geol. Assoc. Can. – Mineral. Assoc. Can., GeoCanada 2000 Conference CD (extended abstr.)*, file 374.pdf.
- RIMSKAYA-KORSAKOVA, O.M., KRASNOVA, N.I. & KOPYLOVA, L.N. (1979): Typical chemical features of apatite from the Kovdor complex deposit. *Mineral. Geokhim.* **6**, 58-70 (in Russ.).
- SANTOS, R.V. & CLAYTON, R.N. (1995): Variations of oxygen and carbon isotopes in carbonatites: a study of Brazilian alkaline complexes. *Geochim. Cosmochim. Acta* **59**, 1339-1352.
- SHARMA, T. & CLAYTON, R.N. (1965): Measurement of O¹⁸/O¹⁶ ratios of total oxygen of carbonates. *Geochim. Cosmochim. Acta* **29**, 1347-1353.
- SITNIKOVA, M.A., ZAITSEV, A.N., WALL, F., CHAKHMOURADIAN, A.R. & SUBBOTIN, V.V. (2000): Evolution of chemical composition of rock-forming carbonates in Sallanlatvi carbonatites, Kola Peninsula, Russia. *In Carbonatites 2000: Genève et Minéralisations Associées*, Abstr., 44.
- SOKOLOV, S.V. (1985): Carbonates in ultramafite, alkali-rock, and carbonatite intrusions. *Geochem. Int.* **22**(4), 150-166.
- SUBBOTIN, V.V., VOLOSHIN, A.V., PAKHOMOVSKY, YA.A. & BAKHCHISARAITSEV, A.YU. (1999): Calcioburbankite and burbankite from carbonatites of the Vuoriyarvi massif (new data). *Zap. Vser. Mineral. Obshchest.* **121**(1), 78-87 (in Russ.).
- TAYLOR, H.P., JR., FRECHEN, J. & DEGENS, E.T. (1967): Oxygen and carbon isotope studies of carbonatites from Laacher See district, West Germany and the Alnö district, Sweden. *Geochim. Cosmochim. Acta* **31**, 407-430.
- VEKSLER, I.V., NIELSEN, T.F.D. & SOKOLOV, S.V. (1998): Mineralogy of crystallized melt inclusions from Gardiner and Kovdor ultramafic alkaline complexes: implications for carbonatite genesis. *J. Petrol.* **39**, 2015-2031.
- WALL, F., BARREIRO, B.A. & SPIRO, B. (1994): Isotopic evidence for late-stage processes in carbonatites: rare earth mineralization in carbonatites and quartz rocks at Kangankunde, Malawi. *Mineral. Mag.* **58A**, 951-952.
- _____ & MARIANO, A.N. (1996): Rare earth minerals in carbonatites: a discussion centred on the Kangankunde carbonatite, Malawi. *In Rare Earth Minerals: Chemistry, Origin and Ore Deposits* (A.P. Jones, F. Wall & C.T. Williams, eds.). *Mineralogical Soc., Ser. 7*. Chapman and Hall, London, U.K. (193-225).
- _____, ZAITSEV, A.N. & MARIANO, A.N. (2000): Rare earth pegmatites in carbonatites. *In Carbonatites 2000: Genève et Minéralisations Associées*, Abstracts, 45.
- ZAITSEV, A.N. (1996): Rhombohedral carbonates from carbonatites of the Khibina massif, Kola Peninsula, Russia. *Can. Mineral.* **34**, 453-468.
- _____ & BELL, K. (1995): Sr and Nd isotope data of apatite, calcite and dolomite as indicators of source, and the relationships of phoscorites and carbonatites from the Kovdor Massif, Kola Peninsula, Russia. *Contrib. Mineral. Petrol.* **121**, 324-335.
- _____, DEMÉNY, A., SINDERN, S. & WALL, F. (2001): Origin of REE mineralization in the Khibina and Vuoriyarvi carbonatites (Kola, Russia) – evidence from a C–O and Sr–Nd isotope study. *In EUG XI 2001 Conference CD* (in press).
- _____, PAVLOV, V.P. & POLEZHAIEVA, L.I. (1990): Apatite mineralization associated with carbonatite complex of the Khibina alkaline massif. *In Alkaline Magmatism of North-East Part of the Baltic Shield* (T.N. Ivanova, ed.). Kola Science Center, Russian Academy of Science, Apatity, Russia, 97-105 (in Russ.).
- _____, WALL, F. & LE BAS, M.J. (1998): REE–Sr–Ba minerals from the Khibina carbonatites, Kola Peninsula, Russia: their mineralogy, paragenesis and evolution. *Mineral. Mag.* **62**, 225-250.

Received March 31, 2001, revised manuscript accepted January xx, 2002.